TUDelft

Delft University of Technology

A Delayed and Subsampled Wideband Sparse Array for Joint Angle and Frequency Estimation

Wang, Feiyu; Leus, Geert

Important note
To cite this publication, please use the final published version (if applicable).
Please check the document version above.

A Delayed and Subsampled Wideband Sparse Array for Joint Angle and Frequency Estimation

Feiyu Wang and Geert Leus, *Fellow, IEEE*

Department of Microelectronics, Delft University of Technology

Delft, The Netherlands

Abstract— In this paper we consider the problem of joint wideband spectrum sensing and direction-of-arrival (DoA) estimation, where a number of uncorrelated narrowband sources spread over a wide frequency band impinge on a sparse linear array (SLA). To overcome the sampling rate bottleneck for wideband spectrum sensing, we rely on sub-Nyquist sampling for the receiver, and to resolve the sources both in the angle and frequency domain, an additional delayed branch is included for every antenna to gain an extra degree of freedom (DoF). Appropriately designing the delays at the different antennas allows us to use the contemporary machinery of co-array processing. We accordingly propose a joint eigenvalue decomposition (EVD) based algorithm to jointly estimate the angles and frequencies of the different sources with automatic pairing. Furthermore, as a consequence of the co-array processing, we can handle more sources than the number of physical antennas. Simulation results are included to corroborate our findings.

Index Terms— Wideband spectrum sensing, direction-of-arrival (DoA) estimation, sub-Nyquist sampling, sparse linear array (SLA), joint eigenvalue decomposition (EVD).

I. INTRODUCTION

Wideband spectrum sensing aims to identify the frequency occupation of a number of narrowband transmissions in a wide frequency band, and has attracted considerable attention in some applications, such as cognitive radio [1], [2], and electronic warfare surveillance [3]. A major technical challenge for wideband spectrum sensing is the need of a high-speed analog-to-digital converter (ADC) to sample the wideband signal at Nyquist rate, which may be infeasible if the spectrum under monitoring is very wide. To overcome this sampling rate bottleneck, plenty of state-of-the-art sub-Nyquist sampling based methods, e.g. [4], [5], were developed. The basic idea in these works is to exploit the inherent sparsity in the frequency domain and to recover the complete wideband signal with only compressed measurements, based on the compressed sensing theory [6].

In some applications such as spectrum surveillance, to facilitate the subsequent signal estimation and analysis, one need not only perform spectrum sensing, but also identify the carrier frequencies and directions-of-arrival (DoAs) associated with the narrowband signals that live within the wide frequency band [7]. However, most existing methods for joint carrier frequency and DoA estimation rely on a Nyquist sampling framework [8], [9]. Recently, to release the ADCs from the extremely high Nyquist sampling rate burden, the sparsity

property in the spectral and spatial domains was exploited to devise sub-Nyquist sampling-based algorithms for joint wideband spectrum sensing and DoA estimation [10]–[14]. Specifically, in [10]–[13] a 1-D linear array is deployed along with time delay-based, or multicoset sampling-based sub-Nyquist sampling architectures, while in [14] an L-shaped array with a modulated wideband converter (MWC) channel for each antenna was designed. Note that in the architecture in [12], [13], a single uniform linear array (ULA) is employed and the received signal at each antenna is first delayed by a flexible time shift and then sampled at a sub-Nyquist sampling rate. Hence only one ADC is required for each antenna output, which leads to a lower hardware complexity compared with the state-of-the-art. However, with this architecture, we still lack the capability of recovering more sources than the number of physical antennas.

In this paper, we extend our previous work [13], to a sparse linear array (SLA) framework for joint wideband spectrum sensing and DoA estimation. Our goal is to resolve more sources than the number of physical antennas, through considering joint temporal and spatial compressed sampling. We do this by constructing a new difference co-array with more degrees of freedom (DoF) than that directly obtained from the physical SLA. In our proposed receiver architecture, the output of each antenna of the SLA has two channels, where one is a direct path and the other is a delayed path with pre-specified delay factors. Each path is followed by a single ADC with a sub-Nyquist sampling rate. Through a proper design of the delay factors, we can calculate a set of cross-correlations of the sub-Nyquist sampled signals, based on which the difference co-array response matrices are formulated to enhance the effective number of DoF of the array. Accordingly, a joint eigenvalue decomposition (EVD) based algorithm is proposed to jointly recover the DoA, carrier frequency, and power spectrum associated with each source, which furthermore allows for an automatic pairing of the estimates. Simulation results show that the proposed method outperforms the state-of-the-art methods, and can handle more sources than the number of physical antennas.

II. PROBLEM FORMULATION

Consider a scenario in which K uncorrelated, wide-sense stationary narrowband signals spread over a wide frequency band. Let $s(t)$ denote the combination of the K narrowband
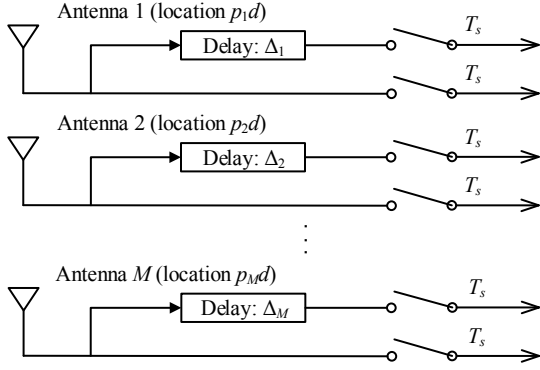
Fig. 1: Proposed sub-Nyquist sampling based wideband receiver architecture.

signals in the time domain. Then $s(t)$ can be expressed as

$$s(t) = \sum_{k=1}^{K} s_k(t) e^{j\omega_k t} \qquad (1)$$

where $s_k(t)$ and $\omega_k \in \mathbb{R}^+$ denote the complex baseband signal and the carrier frequency (in radians per second) of the kth source signal, respectively. We have the following assumptions regarding the source signals:

A1 The K source signals $\{s_k(t)\}$ are assumed to be mutually uncorrelated, wide-sense stationary, and bandlimited to $[-B/2, B/2]$, i.e. $B_k \leq B$, $\forall k$, where B_k denotes the bandwidth of the kth source signal.

A2 The multi-band signal $s(t)$ is bandlimited to $\mathcal{F} = [-f_{\mathrm{nyq}}/2, f_{\mathrm{nyq}}/2]$, and we assume $f_{\mathrm{nyq}} \gg B$.

A3 The bandwidth of each source signal is relatively narrow compared to its carrier frequency, i.e. $\omega_k \gg B$, $\forall k$.

The K source signals are in the far-field of the receiver, which is equipped with a wideband SLA of M antennas. After collecting the received signal at the array, our objective is to jointly estimate the DoAs $\{\theta_k\}$, the carrier frequencies $\{\omega_k\}$, as well as the power spectra associated with the K source signals.

III. PROPOSED SUB-NYQUIST RECEIVER ARCHITECTURE

As noted in the previous section, the cognitive receiver is equipped with a wideband SLA of M antennas. The location of the mth antenna is $p_m d$ where $p_m \in \mathbb{N}$ and d denotes the basic element spacing. The index set of the physical array

$$\mathcal{D}_{\mathrm{phy}} \triangleq \{p_1, p_2, \ldots, p_M\} \qquad (2)$$

is referred to as the spatial sampling pattern of the receiver where $p_1 = 0$ and $p_1 < p_2 < \cdots < p_M$. The largest number of consecutive antennas (with spacing d) in the physical array is denoted as

$$Q_{\mathrm{phy}} \triangleq \arg \max_{\{0,\ldots,Q-1\} \subseteq \mathcal{D}_{\mathrm{phy}}} Q \qquad (3)$$

Under the concept of the co-array equivalence, we define the virtual antenna indices of the difference co-array as

$$\mathcal{D}_{\mathrm{co}} \triangleq \{p_i - p_j : i, j = 1, \ldots, M\} \qquad (4)$$

and the largest number of consecutive antennas (with spacing d) in the virtual array as

$$Q_{\mathrm{co}} \triangleq \arg \max_{\{-Q,\ldots,Q\} \subseteq \mathcal{D}_{\mathrm{co}}} Q \qquad (5)$$

Denote $\{\eta_m\}_{m=1}^{M_{\mathrm{co}}}$ as the elements of $\mathcal{D}_{\mathrm{co}}$ where $\eta_1 < \eta_2 < \cdots < \eta_{M_{\mathrm{co}}}$ with M_{co} being the cardinality of $\mathcal{D}_{\mathrm{co}}$.

In our receiver architecture, the output of the mth antenna has two channels. One is a direct path and the other is a delayed path with pre-specified delay Δ_m. In each channel, the analog signal is sampled by a synchronous ADC with a sampling rate of $f_s = 1/T_s$, where $f_s \ll f_{\mathrm{nyq}}$. We have the following assumptions regarding the delay factors and the sampling rate:

A4 The time delay factors $\{\Delta_m\}_{m=1}^M$ satisfy the following condition

$$\Delta_i - \Delta_j = (p_i - p_j)\Delta, \quad \forall i, j \in \{1, \ldots, M\} \qquad (6)$$

where $\Delta \in \mathbb{R}^+$ satisfies

$$|\Delta f_{\mathrm{nyq}}| < 1. \qquad (7)$$

A5 The sampling rate of each ADC f_s is no less than the bandwidth of the narrowband source signal which has the largest bandwidth among all sources, i.e. $f_s \geq B$.

As will be shown later in our paper, Assumption A4 is essential to identify the unknown carrier frequencies. The proposed receiver architecture is illustrated in Fig. 1. Note that compared with the receiver architecture in [13], here a delayed branch is added for every antenna to gain an extra DoF to resolve the sources both in the angle and frequency domain, from a co-array processing perspective. This point will be further explained at the corresponding parameter estimation stage. The analog signal observed by the delay path of the mth antenna can be expressed as

$$\begin{aligned} \tilde{x}_m(t) &= \sum_{k=1}^{K} s_k(t - p_m \tau_k - \Delta_m) \\ &\quad \times e^{j\omega_k(t - p_m \tau_k - \Delta_m)} + \tilde{w}_m(t) \\ &\approx \sum_{k=1}^{K} s_k(t) e^{j\omega_k(t - p_m \tau_k - \Delta_m)} + \tilde{w}_m(t) \qquad (8) \end{aligned}$$

where $\tilde{w}_m(t)$ represents the zero mean additive white Gaussian noise, and τ_k denotes the delay between two adjacent sensors (with spacing d) for a plane wave arriving in the direction θ_k which is given by

$$\tau_k = \frac{d \cos \theta_k}{C}. \qquad (9)$$

We further assume

A6 The smallest distance between two adjacent antennas d satisfies $d < C/(2f_{\mathrm{nyq}})$, where C is the speed of light.

This assumption is essential for the recovery of the DoAs $\{\theta_k\}$ given $\{\tau_k\}$. The approximation in (8) is due to the narrowband assumption of the source signals $\{s_k(t)\}$ which can be formalized as $B[p_M d/C + \max_m \{\Delta_m\}] \ll 1$.

1635

Similar to the above description, the analog signal observed by the direct path of the mth antenna can be expressed as

$$\bar{x}_m(t) \approx \sum_{k=1}^{K} s_k(t) e^{j\omega_k(t - p_m \tau_k)} + \bar{w}_m(t) \qquad (10)$$

where $\bar{w}_m(t)$ denotes the zero mean additive white Gaussian noise with the same distribution but independent of the noise $\tilde{w}_m(t)$. In the following two sections, we will investigate the cross-correlations between the outputs of the sampling channels, and propose an effective joint EVD-based method to perform joint wideband spectrum sensing and DoA estimation.

IV. THE CROSS-CORRELATION EVALUATION

A. Signal Model

Defining $\tilde{\boldsymbol{a}}_k \triangleq \begin{bmatrix} e^{-j\omega_k(p_1 \tau_k - \Delta_1)} & \dots & e^{-j\omega_k(p_M \tau_k - \Delta_M)} \end{bmatrix}^T$ and $\bar{\boldsymbol{a}}_k \triangleq \begin{bmatrix} e^{-j\omega_k(p_1 \tau_k)} & \dots & e^{-j\omega_k(p_M \tau_k)} \end{bmatrix}^T$, (8) and (10) can be written in a matrix-vector form as

$$\tilde{\boldsymbol{x}}_n = \tilde{\boldsymbol{A}} \boldsymbol{s}_n + \tilde{\boldsymbol{w}}_n, \ n \in \mathbb{N} \qquad (11)$$

$$\bar{\boldsymbol{x}}_n = \bar{\boldsymbol{A}} \boldsymbol{s}_n + \bar{\boldsymbol{w}}_n, \ n \in \mathbb{N} \qquad (12)$$

where

$$\tilde{\boldsymbol{x}}_n \triangleq [\tilde{x}_1(nT_s) \ \dots \ \tilde{x}_M(nT_s)]^T$$
$$\bar{\boldsymbol{x}}_n \triangleq [\bar{x}_1(nT_s) \ \dots \ \bar{x}_M(nT_s)]^T$$
$$\tilde{\boldsymbol{w}}_n \triangleq [\tilde{w}_1(nT_s) \ \dots \ \tilde{w}_M(nT_s)]^T$$
$$\bar{\boldsymbol{w}}_n \triangleq [\bar{w}_1(nT_s) \ \dots \ \bar{w}_M(nT_s)]^T$$
$$\tilde{\boldsymbol{A}} \triangleq [\tilde{\boldsymbol{a}}_1 \ \dots \ \tilde{\boldsymbol{a}}_K], \ \bar{\boldsymbol{A}} \triangleq [\bar{\boldsymbol{a}}_1 \ \dots \ \bar{\boldsymbol{a}}_K] \qquad (13)$$

and

$$\boldsymbol{s}_n \triangleq \begin{bmatrix} s_1(nT_s) e^{j\omega_1(nT_s)} & \dots & s_K(nT_s) e^{j\omega_K(nT_s)} \end{bmatrix}^T \qquad (14)$$

From Assumption A1, we know that the K sources are mutually uncorrelated and wide-sense stationary, and thus we have

$$\mathbb{E}\left[\boldsymbol{s}_{n+l} \boldsymbol{s}_n^H\right] = \text{diag}\{\boldsymbol{r}^s(l)\}, \ l \in \{-L, \dots, L\} \qquad (15)$$

where $\mathbb{E}[\cdot]$ represents the expectation operator, $\boldsymbol{r}^s(l) \triangleq [r_1^s(l) \ \dots \ r_K^s(l)]^T$ and

$$r_k^s(l) \triangleq \mathbb{E}\left[s_k(t + lT_s) e^{j\omega_k(t + lT_s)} s_k^*(t) e^{-j\omega_k t}\right] \qquad (16)$$

denotes the autocorrelation of the kth modulated source signal, with $(\cdot)^*$ standing for the complex conjugate. Regarding the noise terms, we assume

$$\mathbb{E}\left[\tilde{\boldsymbol{w}}_{n+l} \tilde{\boldsymbol{w}}_n^H\right] = \mathbb{E}\left[\bar{\boldsymbol{w}}_{n+l} \bar{\boldsymbol{w}}_n^H\right] = \delta(l) \cdot \sigma^2 \boldsymbol{I}_M \qquad (17)$$

where σ^2 represents the noise power, $\boldsymbol{I}_m$ denotes an $m \times m$ identity matrix, and $\delta(l)$ is the Kronecker delta function which returns 1 for $l = 0$, and 0 otherwise. Also, due to the fact that $\tilde{w}_m(t)$ and $\bar{w}_m(t)$ are mutually independent we have

$$\mathbb{E}\left[\tilde{\boldsymbol{w}}_{n+l} \bar{\boldsymbol{w}}_n^H\right] = \boldsymbol{0}_{M,M}, \ \forall n, l \in \mathbb{N} \qquad (18)$$

with $\boldsymbol{0}_{m,n}$ denoting an $m \times n$ matrix of zeros. Based on the above signal model, we will calculate the cross-correlations of the sampled signals in the following subsection.

B. Cross-Correlation

Regarding the cross-correlation between the two delayed channel outputs $\tilde{\boldsymbol{x}}_{n+l}$ and $\tilde{\boldsymbol{x}}_n$, recalling Assumption A1 and (15)-(17), we have

$$\mathbb{E}\left[\tilde{\boldsymbol{x}}_{n+l} \tilde{\boldsymbol{x}}_n^H\right] = \tilde{\boldsymbol{A}} \cdot \mathbb{E}\left[\boldsymbol{s}_{n+l} \boldsymbol{s}_n^H\right] \cdot \tilde{\boldsymbol{A}}^H + \mathbb{E}\left[\tilde{\boldsymbol{w}}_{n+l} \tilde{\boldsymbol{w}}_n^H\right]$$
$$= \tilde{\boldsymbol{A}} \cdot \text{diag}\{\boldsymbol{r}^s(l)\} \cdot \tilde{\boldsymbol{A}}^H + \delta(l) \cdot \sigma^2 \boldsymbol{I}_M \qquad (19)$$

Vectorizing this expression, we obtain

$$\text{vec}\left(\mathbb{E}\left[\tilde{\boldsymbol{x}}_{n+l} \tilde{\boldsymbol{x}}_n^H\right]\right) = \left(\tilde{\boldsymbol{A}}^* \circ \tilde{\boldsymbol{A}}\right) \boldsymbol{r}^s(l) + \delta(l) \cdot \sigma^2 \text{vec}\left(\boldsymbol{I}_M\right)$$

where $\circ$ stands for the Khatri-Rao product. From Assumption A4, i.e., with the special design of the time delay factors $\{\Delta_m\}_{m=1}^M$ in (6), the $(M(m_2 - 1) + m_1, k)$th entry of the new array response matrix $\left(\tilde{\boldsymbol{A}}^* \circ \tilde{\boldsymbol{A}}\right) \in \mathbb{C}^{M^2 \times K}$, $\forall m_1, m_2 \in \{1, \dots, M\}$, can be expressed as

$$e^{-j\omega_k\left[(p_{m_1} - p_{m_2})\tau_k + (\Delta_{m_1} - \Delta_{m_2})\right]} = e^{-j\omega_k(\tau_k + \Delta)(p_{m_1} - p_{m_2})}$$

The above equation illustrates that each row of the new array response matrix $\left(\tilde{\boldsymbol{A}}^* \circ \tilde{\boldsymbol{A}}\right)$ is only parameterized by a specific index $\eta_m \in \mathcal{D}_{\text{co}}$, $m = 1, \dots, M_{\text{co}}$, which represents the difference of the antenna locations of the physical array. After averaging the repeated rows in $\left(\tilde{\boldsymbol{A}}^* \circ \tilde{\boldsymbol{A}}\right)$ and the related entries in $\text{vec}\left(\mathbb{E}\left[\tilde{\boldsymbol{x}}_{n+l} \tilde{\boldsymbol{x}}_n^H\right]\right)$, we have

$$\tilde{\boldsymbol{r}}^x(l) \triangleq \boldsymbol{J} \cdot \text{vec}\left(\mathbb{E}\left[\tilde{\boldsymbol{x}}_{n+l} \tilde{\boldsymbol{x}}_n^H\right]\right)$$
$$= \boldsymbol{B}(\Delta) \boldsymbol{r}^s(l) + \boldsymbol{r}^w(l), \qquad (20)$$

where $\boldsymbol{J} \in \{0, 1/n : \ n \in \mathbb{N}^+\}^{M_{\text{co}} \times M^2}$ is the corresponding select-and-average matrix, $\boldsymbol{r}^w(l) \triangleq \delta(l)\sigma^2 \boldsymbol{J} \text{vec}\left(\boldsymbol{I}_M\right)$, and

$$\boldsymbol{B}(\Delta) \triangleq \boldsymbol{J} \cdot \left(\tilde{\boldsymbol{A}}^* \circ \tilde{\boldsymbol{A}}\right) \in \mathbb{C}^{M_{\text{co}} \times K} \qquad (21)$$

is the (non-redundant) co-array response matrix related to the delayed channels. The kth column of $\boldsymbol{B}(\Delta)$ can be expressed as $\boldsymbol{b}_k(\Delta) \triangleq [b_{1,k}(\Delta) \ \dots \ b_{M_{\text{co}},k}(\Delta)]^T$, with

$$b_{m,k}(\Delta) \triangleq e^{-j\eta_m \omega_k(\tau_k + \Delta)}. \qquad (22)$$

Similarly, for the cross-correlation between the two direct channel outputs $\bar{\boldsymbol{x}}_{n+l}$ and $\bar{\boldsymbol{x}}_n$, we have

$$\mathbb{E}\left[\bar{\boldsymbol{x}}_{n+l} \bar{\boldsymbol{x}}_n^H\right] = \bar{\boldsymbol{A}} \cdot \text{diag}\{\boldsymbol{r}^s(l)\} \cdot \bar{\boldsymbol{A}}^H + \delta(l) \cdot \sigma^2 \boldsymbol{I}_M \qquad (23)$$

Vectorizing the above expression and averaging the related entries, we get

$$\bar{\boldsymbol{r}}^x(l) \triangleq \boldsymbol{J} \cdot \text{vec}\left(\mathbb{E}\left[\bar{\boldsymbol{x}}_{n+l} \bar{\boldsymbol{x}}_n^H\right]\right)$$
$$= \boldsymbol{B}(0) \boldsymbol{r}^s(l) + \boldsymbol{r}^w(l), \qquad (24)$$

where $\boldsymbol{B}(0) \in \mathbb{C}^{M_{\text{co}} \times K}$ is the (non-redundant) co-array response matrix related to the direct channels, and is defined as in (21) and (22) with $\Delta = 0$.

The cross-correlation between the delayed and direct channel outputs, i.e., $\tilde{\boldsymbol{x}}_{n+l}$ and $\bar{\boldsymbol{x}}_n$, can be computed as

$$\mathbb{E}\left[\tilde{\boldsymbol{x}}_{n+l} \bar{\boldsymbol{x}}_n^H\right] = \tilde{\boldsymbol{A}} \cdot \mathbb{E}\left[\boldsymbol{s}_{n+l} \boldsymbol{s}_n^H\right] \cdot \bar{\boldsymbol{A}}^H + \mathbb{E}\left[\tilde{\boldsymbol{w}}_{n+l} \bar{\boldsymbol{w}}_n^H\right]$$
$$= \tilde{\boldsymbol{A}} \cdot \text{diag}\{\boldsymbol{r}^s(l)\} \cdot \bar{\boldsymbol{A}}^H \qquad (25)$$

1636

Note that in (25) the cross-correlation of the noise terms is totally nulled out due to (18). Vectorizing (25), we obtain

$$\boldsymbol{r}^{\tilde{x}\bar{x}}(l) \triangleq \text{vec}\left(\mathbb{E}\left[\tilde{\boldsymbol{x}}_{n+l}\bar{\boldsymbol{x}}_n^H\right]\right) = \left(\bar{\boldsymbol{A}}^* \odot \tilde{\boldsymbol{A}}\right) \cdot \boldsymbol{r}^s(l) \qquad (26)$$

Given the second-order statistics $\{\tilde{\boldsymbol{r}}^x(l)\}_{l=-L}^{+L}$, $\{\bar{\boldsymbol{r}}^x(l)\}_{l=-L}^{+L}$ and $\{\boldsymbol{r}^{\tilde{x}\bar{x}}(l)\}_{l=-L}^{+L}$, our objective is to recover the DoAs $\{\theta_k\}$, the carrier frequencies $\{\omega_k\}$, as well as the power spectra associated with the K source signals.

V. PARAMETER ESTIMATION

Denote $\boldsymbol{r}(l) \triangleq \left[(\tilde{\boldsymbol{r}}^x(l))^T \ (\bar{\boldsymbol{r}}^x(l))^T \ (\boldsymbol{r}^{\tilde{x}\bar{x}}(l))^T\right]^T$ and $\boldsymbol{Y} \triangleq \left[\boldsymbol{r}(-L) \ \ldots \ \boldsymbol{r}(L)\right]$. Considering the noiseless case for simplicity, $\boldsymbol{Y}$ can be written as

$$\boldsymbol{Y} = \begin{bmatrix} \boldsymbol{B}(\Delta) \\ \boldsymbol{B}(0) \\ \bar{\boldsymbol{A}}^* \odot \tilde{\boldsymbol{A}} \end{bmatrix} \cdot \boldsymbol{R}^s \qquad (27)$$

where $\boldsymbol{R}^s \triangleq \left[\boldsymbol{r}^s(-L) \ \ldots \ \boldsymbol{r}^s(L)\right]$. Assuming the number of sources, K, is known or estimated *a priori*, then the singular value decomposition (SVD) of $\boldsymbol{Y}$ yields

$$\boldsymbol{Y} = [\boldsymbol{U}_s \ \boldsymbol{U}_w] \boldsymbol{\Lambda} [\boldsymbol{V}_s \ \boldsymbol{V}_w]^H \qquad (28)$$

where $\boldsymbol{\Lambda}$ is a $(2M_{\text{co}} + M^2) \times (2L + 1)$ rectangular diagonal matrix, $\{\boldsymbol{U}_s, \boldsymbol{V}_s\}$ and $\{\boldsymbol{U}_w, \boldsymbol{V}_w\}$ represent the signal and noise subspace, respectively. With a similar derivation as in the classical ESPRIT [15], we have

$$\boldsymbol{U}_s = \begin{bmatrix} \boldsymbol{B}(\Delta) \\ \boldsymbol{B}(0) \\ \bar{\boldsymbol{A}}^* \odot \tilde{\boldsymbol{A}} \end{bmatrix} \cdot \boldsymbol{T} \qquad (29)$$

where $\boldsymbol{T}$ is a nonsingular transformation matrix. We see that the information about the parameters $\{\theta_k\}$ and $\{\omega_k\}$ can be extracted from $\boldsymbol{U}_s$. To extract them, we follow the next procedure. Denote $\mathcal{S}_{\text{phy}} = \{1, \ldots, Q_{\text{phy}}\}$ and $\mathcal{S}_{\text{co}} = \{-Q_{\text{co}} + \frac{M_{\text{co}}+1}{2}, \ldots, Q_{\text{co}} + \frac{M_{\text{co}}+1}{2}\}$ as the indexes of the sub-array with the largest number of consecutive antennas of respectively the physical array and the difference co-array. Define the selection matrix $\boldsymbol{J}_m(\mathcal{S}) \in \{0, 1\}^{|\mathcal{S}| \times m}$ which picks the entries of a vector according to the indexes in $\mathcal{S}$, with $|\mathcal{S}|$ the cardinality of $\mathcal{S}$. Now define four selection matrices as

$$\boldsymbol{G}_{11} \triangleq \text{blkdiag}\left\{\left[\boldsymbol{J}_1 \ \boldsymbol{0}_{(M_{\text{co}}-1),M_{\text{co}}}\right], \ \boldsymbol{J}_{11}\right\} \qquad (30)$$

$$\boldsymbol{G}_{12} \triangleq \text{blkdiag}\left\{\left[\boldsymbol{J}_2 \ \boldsymbol{0}_{(M_{\text{co}}-1),M_{\text{co}}}\right], \ \boldsymbol{J}_{12}\right\} \qquad (31)$$

$$\boldsymbol{G}_{21} \triangleq \text{blkdiag}\left\{\left[\boldsymbol{0}_{(M_{\text{co}}-1),M_{\text{co}}} \ \boldsymbol{J}_1\right], \ \boldsymbol{J}_{21}\right\} \qquad (32)$$

$$\boldsymbol{G}_{22} \triangleq \text{blkdiag}\left\{\left[\boldsymbol{0}_{(M_{\text{co}}-1),M_{\text{co}}} \ \boldsymbol{J}_2\right], \ \boldsymbol{J}_{22}\right\} \qquad (33)$$

where

$$\boldsymbol{J}_1 \triangleq \boldsymbol{J}_{M_{\text{co}}}\left(\mathcal{S}_{\text{co}} \backslash \left\{Q_{\text{co}} + \frac{M_{\text{co}}+1}{2}\right\}\right)$$

$$\boldsymbol{J}_2 \triangleq \boldsymbol{J}_{M_{\text{co}}}\left(\mathcal{S}_{\text{co}} \backslash \left\{-Q_{\text{co}} + \frac{M_{\text{co}}+1}{2}\right\}\right)$$

$$\boldsymbol{J}_{11} \triangleq \boldsymbol{I}_M \otimes \boldsymbol{J}_M\left(\mathcal{S}_{\text{phy}} \backslash \{Q_{\text{phy}}\}\right)$$

$$\boldsymbol{J}_{12} \triangleq \boldsymbol{I}_M \otimes \boldsymbol{J}_M\left(\mathcal{S}_{\text{phy}} \backslash \{1\}\right)$$

$$\boldsymbol{J}_{21} \triangleq \boldsymbol{J}_M\left(\mathcal{S}_{\text{phy}} \backslash \{Q_{\text{phy}}\}\right) \otimes \boldsymbol{I}_M$$

$$\boldsymbol{J}_{22} \triangleq \boldsymbol{J}_M\left(\mathcal{S}_{\text{phy}} \backslash \{1\}\right) \otimes \boldsymbol{I}_M$$

Following the strategy of ESPRIT, we have

$$\boldsymbol{\Gamma}_1 \triangleq \left(\boldsymbol{G}_{11}\boldsymbol{U}_s\right)^\dagger \left(\boldsymbol{G}_{12}\boldsymbol{U}_s\right) = \boldsymbol{T}^{-1}\boldsymbol{\Psi}_1\boldsymbol{T} \qquad (34)$$

$$\boldsymbol{\Gamma}_2 \triangleq \left(\boldsymbol{G}_{21}\boldsymbol{U}_s\right)^\dagger \left(\boldsymbol{G}_{22}\boldsymbol{U}_s\right) = \boldsymbol{T}^{-1}\boldsymbol{\Psi}_2\boldsymbol{T} \qquad (35)$$

where

$$\boldsymbol{\Psi}_1 = \text{diag}\{e^{-j\omega_1(\tau_1+\Delta)}, \ldots, e^{-j\omega_K(\tau_K+\Delta)}\} \qquad (36)$$

$$\boldsymbol{\Psi}_2 = \text{diag}\{e^{-j\omega_1\tau_1}, \ldots, e^{-j\omega_K\tau_K}\} \qquad (37)$$
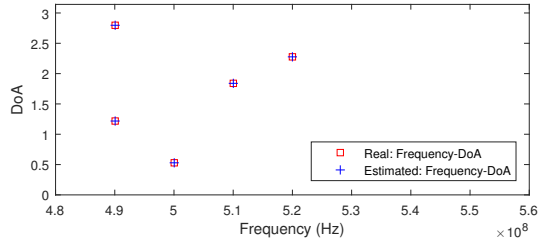
Obviously, a joint EVD [16]–[18] can be performed on the matrices $\{\boldsymbol{\Gamma}_1, \boldsymbol{\Gamma}_2\}$ to get an estimate of $\boldsymbol{\Psi}_1$ and $\boldsymbol{\Psi}_2$, from which $\{\tau_k\}$ and $\{\omega_k\}$ can be obtained thereafter. Specifically, we first get the estimates of $\{\omega_k\tau_k\}$ from (37), and then resort to (36) to estimate the related $\{\omega_k\}$ and $\{\tau_k\}$. Note that with this joint EVD technique, the estimates of $\{\tau_k\}$ and $\{\omega_k\}$ are paired automatically. The final DoA estimates can be obtained from $\{\tau_k\}$ without ambiguity when Assumption A6 holds, and, given $\{\omega_k\}$, the original power spectra of the sources can be recovered using the approach in [13] as long as Assumptions A1, A2 and A5 hold. It is also noteworthy that if the delayed paths are removed, then (27) reduces to $\boldsymbol{Y} = \boldsymbol{B}(0)\boldsymbol{R}^s$, which makes the joint estimation of $\{\tau_k\}$ and $\{\omega_k\}$ impossible.

Considering the identifiability of our proposed method in the noiseless case, one sufficient condition for the exact recovery of the unknown parameters could be $\text{rank}(\boldsymbol{R}^s) = K$, and $Q_{\text{phy}} > K$ or $(2Q_{\text{co}} + 1) > K$. Noting that even if $K > M$, from the co-array perspective, $(2Q_{\text{co}} + 1) > K$ can still hold, which indicates that we have the capability of performing joint wideband spectrum sensing and DoA estimation with more sources than the number of physical antennas.
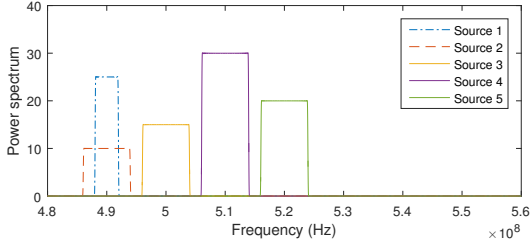
VI. SIMULATION RESULTS

In this section, we carry out a few experiments to illustrate the performance of the proposed sub-Nyquist sampling architecture as well as the joint DoA and frequency estimation method. In our simulations, we set $f_{\text{nyq}} = 1.2$ GHz, and the basic element spacing d is set equal to $d = 0.48 \times C/f_{\text{nyq}}$ in order to meet Assumption A6. A 2-level nested array of $M = 4$ antennas is considered whose index set is $\mathcal{D}_{\text{phy}} = \{0, 1, 2, 5\}$. Note that under this setup, the difference co-array consists of $M_{\text{co}} = 11$ consecutive antennas, which leads to $(2Q_{\text{co}} + 1) = M_{\text{co}}$ and $Q_{\text{co}} = 5$. The time delay factors are set as $\{\Delta_m\}_{m=1}^M = \{p_m\Delta\}_{m=1}^M$ with $\Delta = 0.5 \times 10^{-9}$ s, which allows us to satisfy Assumption A4. The signal-to-noise ratio (SNR) is defined as $\text{SNR} \triangleq \mathbb{E}\left[|s(t)|^2\right]/\sigma^2$.
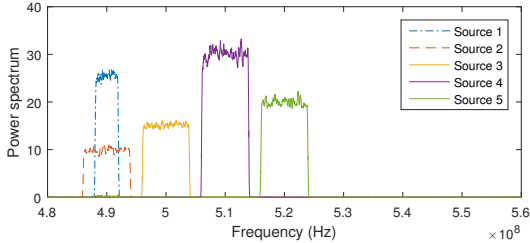
We first consider the case in which $K = 5$ uncorrelated, wide-sense stationary sources spread over the wide frequency band $[-600, 600]$ MHz are received by the aforementioned 2-level nested array. The DoAs of these five sources are given respectively by $\{70, 160, 30, 105, 130\}\pi/180$. The carrier frequencies and bandwidths associated with these sources are set to $\{f_k\}_{k=1}^5 = \{490, 490, 500, 510, 520\}$ MHz, and $\{B_k\}_{k=1}^5 = \{4, 8, 8, 8, 8\}$ MHz. The number of data samples per channel, which is used for calculating the correlation matrices, is set to $N_s = 3 \times 10^5$. The sampling rate f_s is chosen to be $f_s = 80$ MHz and the SNR is set to 40 dB. Fig. 2(a) shows the true (marked with '□') and the estimated (marked with '+') carrier frequencies and DoAs for the five

1637

(a) True and estimated carrier frequencies and DoAs.

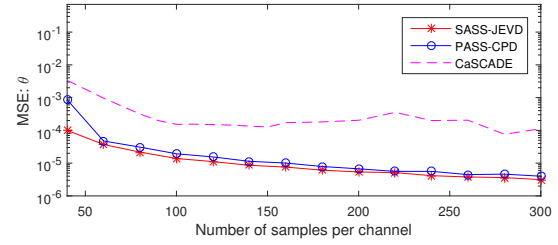(b) Original power spectra of sources.
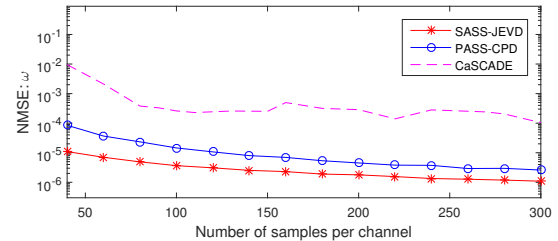

(c) Estimated power spectra of sources.

Fig. 2: Estimated carrier frequencies, DoAs and power spectra for sources that have spectral overlap, SNR = 40 dB.

sources. We can see that the estimated carrier frequencies and DoAs coincide with the groundtruth well. Fig. 2(b) and Fig. 2(c) respectively plot the original power spectrum and the estimated power spectrum of the wide frequency band. It can be observed that our proposed method, even with a sampling rate far below the Nyquist rate, is able to accurately identify the locations of the occupied bands. Furthermore, it could be observed that, although the signals from Sources 1 and 2 overlap each other in the frequency domain, our proposed method still works well.

To better evaluate the performance of our proposed method, we calculate the mean square error (MSE) for the DoAs and the normalized mean square error (NMSE) for the carrier frequencies, which are defined as $\text{MSE}(\theta) = \sum_{k=1}^{K} |\theta_k - \hat{\theta}_k|^2$ and $\text{NMSE}(\omega) = \sum_{k=1}^{K} |\omega_k - \hat{\omega}_k|^2 / |\omega_k|^2$, respectively. In this example, we set the number of sources to $K = 2$. The parameters associated with the two sources are given as: $f_1 = 500$ MHz, $f_2 = 530$ MHz, $\theta_1 = (45/180)\pi$, $\theta_2 = (95/180)\pi$, and $B_k = 8$ MHz, $k = 1, 2$. The sampling rate is set to $f_s = 80$ MHz. Our proposed estimation method is denoted as the Sparse linear Array based Sub-Nyquist Sampling architecture with Joint EVD (SASS-JEVD). We also compare our proposed method with two state-of-the-art sub-

(a) MSE for $\{\theta_k\}$ vs. N_s

(b) NMSE for $\{\omega_k\}$ vs. N_s

Fig. 3: MSE for the DoAs $\{\theta_k\}$ and NMSE for the carrier frequencies $\{\omega_k\}$ vs. the number of samples per channel, where SNR = 30 dB.

Nyquist sampling-based joint angle and frequency estimation methods, namely, the PASS-CPD [13] and the CaSCADE [14]. To make a fair comparison, we assume 8 antennas for PASS-CPD such that its number of sampling channels is identical to that of our architecture. In CaSCADE, an L-shaped array is employed and the number of antennas along each axis is set to 5. Fig. 3 depicts the MSEs/NMSEs of the respective sets of parameters vs. the number of samples per channel N_s, where we set SNR = 30 dB. The results are averaged over 10^3 independent runs, where the baseband complex source signals are randomly generated for each run. It can be observed that our proposed method achieves a much higher carrier frequency and DoA estimation accuracy than the other two methods. This performance improvement is primarily due to the fact that our proposed method utilizes both spatial and temporal correlations of the received signals. Also, in SASS-JEVD, the enhanced DoF from the difference co-array configuration is exploited to get an additional performance gain, while this was neglected in the PASS-CPD.

VII. CONCLUSION

We studied the problem of joint wideband spectrum sensing and DoA estimation with an SLA. To overcome the sampling rate bottleneck for wideband spectrum sensing, we utilized sub-Nyquist sampling for the receiver, and an additional delayed branch was included for every antenna. Then, with a specific design of the delays, co-array processing was employed, and we accordingly proposed a joint EVD based algorithm to jointly estimate the angles and frequencies of the sources with automatic pairing. Simulation results show that our proposed method outperforms the state-of-the-art and can handle more sources than the number of physical antennas.

REFERENCES

[1] E. Axell, G. Leus, E. G. Larsson, and H. V. Poor, "Spectrum sensing for cognitive radio: State-of-the-art and recent advances," *IEEE Signal Processing Magazine*, vol. 29, no. 3, pp. 101–116, May 2012.

[2] H. Sun, A. Nallanathan, C.-X. Wang, and Y. Chen, "Wideband spectrum sensing for cognitive radio networks: a survey," *IEEE Wireless Communications*, vol. 20, no. 2, pp. 74–81, Apr. 2013.

[3] A. Spezio, "Electronic warfare systems," *IEEE Transactions on Microwave Theory and Techniques*, vol. 50, no. 3, pp. 633–644, Mar. 2002.

[4] M. Mishali and Y. C. Eldar, "From theory to practice: Sub-Nyquist sampling of sparse wideband analog signals," *IEEE J. Sel. Topics Signal Process.*, vol. 4, no. 2, pp. 375–391, Apr. 2010.

[5] M. Mishali, Y. C. Eldar, O. Dounaevsky, and E. Shoshan, "Xampling: Analog to digital at sub-Nyquist rates," *IET Circuits, Devices and Systems*, vol. 5, no. 1, pp. 8–20, Jan. 2011.

[6] D. L. Donoho, "Compressive sensing," *IEEE Trans. Information Theory*, vol. 52, no. 4, pp. 1289–1306, Apr. 2006.

[7] M. D. Zoltowski and C. P. Mathews, "Real-time frequency and 2-D angle estimation with sub-Nyquist spatio-temporal sampling," *IEEE Trans. Signal Processing*, vol. 42, no. 10, pp. 2781–2794, Oct. 1994.

[8] A. N. Lemma, A.-J. van der Veen, and E. F. Deprettere, "Joint angle-frequency estimation using multi-resolution ESPRIT," in *IEEE International Conference on Acoustics, Speech, and Signal Processing*, Seattle, Washington, USA, 1998, pp. 1957–1960.

[9] ——, "Analysis of joint angle-frequency estimation using ESPRIT," *IEEE Trans. Signal Processing*, vol. 51, no. 5, pp. 1264–1283, May 2003.

[10] D. D. Ariananda and G. Leus, "Compressive joint angular-frequency power spectrum estimation," in *IEEE European Signal Processing Conference*, Marrakech, Morocco, 2013, pp. 1–5.

[11] A. A. Kumar, S. G. Razul, and C.-M. S. See, "An efficient sub-Nyquist receiver architecture for spectrum blind reconstruction and direction of arrival estimation," in *IEEE International Conference on Acoustics, Speech, and Signal Processing*, Florence, Italy, 2014, pp. 6781–6785.

[12] J. Fang, F. Wang, and H. Li, "Compressed power spectrum, carrier and DOA estimation via PARAFAC decomposition," in *IEEE International Workshop on Computational Advances in Multi-Sensor Adaptive Processing (CAMSAP)*, Curaçao, Dutch Antilles, 2017, pp. 1–4.

[13] F. Wang, J. Fang, H. Duan, and H. Li, "Phased-array-based sub-Nyquist sampling for joint wideband spectrum sensing and direction-of-arrival estimation," *IEEE Trans. Signal Processing*, vol. 66, no. 23, pp. 6110–6123, Dec. 2018.

[14] S. S. Ioushua, O. Yair, D. Cohen, and Y. C. Eldar, "CaSCADE: Compressed carrier and DOA estimation," *IEEE Trans. Signal Processing*, vol. 65, no. 10, pp. 2645–2658, May 2017.

[15] R. Roy and T. Kailath, "ESPRIT-estimation of signal parameters via rotational invariance techniques," *IEEE Trans. Acoust., Speech, Signal Processing*, vol. 37, no. 7, pp. 984–995, July 1989.

[16] M. Zoltowski, M. Haardt, and C. Mathews, "Closed-form 2-D angle estimation with rectangular arrays in element space or beamspace via unitary ESPRIT," *IEEE Trans. Signal Processing*, vol. 44, no. 2, pp. 316–328, Feb. 1996.

[17] A.-J. van der Veen, M. Vanderveen, and A. Paulraj, "Joint angle and delay estimation using shift-invariance techniques," *IEEE Trans. Signal Processing*, vol. 46, no. 2, pp. 405–418, Feb. 1998.

[18] R. André, X. Luciani, and E. Moreau, "Joint EigenValue decomposition algorithms based on first-order Taylor expansion," *IEEE Trans. Signal Processing*, vol. 68, pp. 1716–1727, 2020.